Electronic transmission in quasiperiodic serial stub structures

2004 J. Phys.: Condens. Matter 16 313

(http://iopscience.iop.org/0953-8984/16/3/011)

INSTITUTE OF PHYSICS PUBLISHING JOURNAL OF PHYSICS: CONDENSED MATTER

J. Phys.: Condens. Matter **16** (2004) 313–323 PII: S0953-8984(04)68631-0

Electronic transmission in quasiperiodic serial stub structures

Samar Chattopadhyay[1] **and Arunava Chakrabarti**[2]

[1] Department of Physics, Hooghly Mohsin College, Chinsurah, West Bengal 712 101, India
[2] Department of Physics, University of Kalyani, Kalyani, West Bengal 741 235, India

E-mail: arunava@klyuniv.ernet.in

Received 5 September 2003
Published 9 January 2004
Online at stacks.iop.org/JPhysCM/16/313 (DOI: 10.1088/0953-8984/16/3/011)

Abstract

We present exact results on the electronic transmission through quantum stub waveguides arranged in a Fibonacci quasiperiodic pattern. Discretizing the Schrödinger equation, we map the problem into an equivalent tight binding form and study the transmission spectrum using the transfer matrix method. We emphasize the effect of local positional correlations in a Fibonacci quantum stub array that may lead to resonant eigenstates. Using the real space renormalization group ideas we unravel various local clusters of stubs responsible for resonance. Extended eigenstates have been shown to exist and we find that, under some special circumstances, the electronic charge density exhibits a totally periodic character in such a non-periodic sequence. Our method is completely general and can be applied to any arbitrary sequence of stubs: periodic, quasiperiodic or random. This may lead to a possible experimental verification of the role of positional correlations in the transport behaviour of a class of mesoscopic devices.

1. Introduction

The study of electronic transport through mesoscopic devices has been one of the major areas of research in condensed matter physics in recent times [1–12]. Electrons are transmitted coherently across these systems with negligible inelastic scattering and the phase coherence length is greater than the characteristic device scale length. The latter is of the same order of magnitude as the de Broglie wavelength for mesoscopic systems. The tremendous advances in fabrication techniques has led to the fabrication of a variety of quantum structures such as quantum dots, quantum wires and rings [1–12]. At low temperatures the transport of electrons in such mesoscopic systems is ballistic or quasi-ballistic and resembles the propagation of microwaves through a waveguide. So, the allowed modes may be considered as the waveguide modes and the transport properties are solely determined by the impurity configuration and the geometry of the conductor [13].

The propagation of electrons along quantum wires with various geometric structures has been an interesting problem. Sols *et al* [6] have studied semiconductor stub structures exhibiting transistor functions. They have shown that a small change of stub length changes the transmission spectrum non-trivially. Experiments have also been done to verify the waveguide characteristics of electron transport through a wide–narrow–wide structure by a splitting gate technique [13, 14]. Earlier, Xia [10] proposed a simple one-dimensional waveguide theory for a quantum wire with one or two stubs, and also for a ring with or without a magnetic flux penetrating it. Singha Deo and Jayannavar [11] extended the theory to an assembly of ring and stub structures. They have studied the non-trivial changes in band structure, both for periodic arrays of stubs and a single defect within an otherwise periodic stub arrangement. Shi and Gu [15] studied the quantum waveguide (QWG) transport with side-branch structures and introduced impedance factors for geometric and potential scatterers and developed a recursive algorithm. Simple tight binding results have recently been reported on the formation of electronic bandgaps in a one-dimensional model of nano-wires [16]. The band structure is found to be significantly sensitive to the number of atoms in the side wires, as well as to the periodicity with which the wires are arranged on the backbone. Transmission of electrons through non-interacting model nano-wires with dangling side branches still remains a problem of interest, as has been suggested in some recent work [17, 18]. Partly motivated by these studies, which indicate that the spectral properties of nano-wires with side branches should be sensitive to the geometry of the arrangement, here we address the problem of electron propagation in quasiperiodically ordered stub structures. We apply our theory to investigate the resonant single-particle states and transmission characteristics of a Fibonacci array of stubs. In a couple of recent papers Jin *et al* [19] and Peng *et al* [20] have studied some aspects of electron transport in quasiperiodic quantum waveguides (QWG). However, we look at the problem from a different standpoint. In particular, we make an analytical attempt to unravel the role of positional correlation in the transport properties of a Fibonacci quantum waveguide (FQWG). In a classic golden mean Fibonacci lattice comprised of point-like scatterers the single-particle states are neither localized nor extended in a conventional sense [21–23]. Recently, it has been pointed out [24] that the well known cyclic behaviour of the matrix map in a Fibonacci lattice [21–23] and its variants is basically due to resonance in some local clusters in the lattice which exhibit a *hidden* dimer-like positional correlation. Such 'dimers' are now known to cause resonant or extended eigenstates in an otherwise random lattice [25–27] and even in certain classes of quasiperiodic lattices [28, 29]. It should be mentioned here that one of the early studies regarding the existence of extended wavefunctions in non-translationally invariant one-dimensional quasiperiodic chains is due to Sire and Mosseri [30]. They have nicely discussed the closing of gaps in the energy spectrum and the vanishing invariant and have related these to the existence of extended eigenstates on rational approximants of general quasiperiodic chains, which include the Fibonacci chain as well. However, for the golden mean Fibonacci chain the dimers referred to earlier appear in a nested fashion, whose presence can be revealed at different scales of length, depending on the energy of the incoming electron and the parameters of the Hamiltonian [24].

In the present work we find that the effect of positional correlation in a FQWG structure can be revealed at different scales of length by tuning the length of the stub. The length of the stub can be controlled by the gate voltage from outside [5, 6]. Therefore, this aspect, to our mind, promises an interesting experimental verification of the role of positional correlations in enhancing dc conductivity in such mesoscopic structures. We also find that there are extended eigenstates in a FQWG structure. Some of these states are completely periodic in nature. The situation is easily contrasted to a purely 1D Fibonacci structure with point-like objects, where all the eigenstates are critical [21–23]. We have been able to work out the conditions under

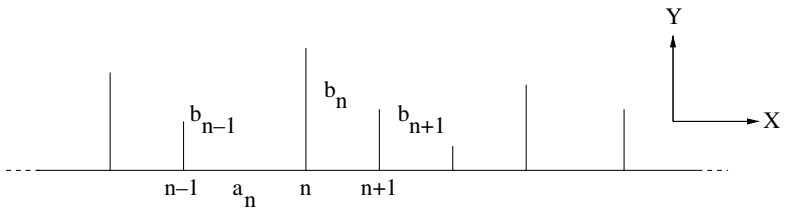

Figure 1. General representation of a one-dimensional stub structure.

which a FQWG array will support such extended eigenstates. Our work is based on the transfer matrix formalism and real space renormalization group (RSRG) method. For implementing the latter, we have mapped the continuous version of the Schrödinger equation into a hierarchy of difference equations, much in the spirit of the Poincaré mapping technique [34], usually done in studying electronic transmission through an array of potential barriers. The discretization allows us to identify the local clusters in a FQWG array, which are responsible for the resonant eigenstates, and are intimately connected to the cycles of the matrix maps exhibited by the sequence. We find that by altering the length of the stubs in a deterministic way we can extract different values of the wavevector for which cycles of the matrix maps are observed. We also present an interesting result which shows that, for some special choices of the stub lengths and their relative separation, one can come across a whole set of values of the wavevector for which the FQWG system exhibits a power-law decay in the transmission coefficient as the system grows in size. Our results are analytical and exact.

In what follows we describe our method and the results. In section 2 we describe the theory of multiple stub structures. Section 3 deals with the Fibonacci array. The resonance conditions are discussed separately for different models. In section 4 we study the transmission properties of a FQWG array. The values of the wavevector for which the transmittivity exhibits a power-law decay as a function of system size is also addressed here. In section 5 we draw some conclusions.

2. The theory of multiple stubs in series

We consider a quantum wire which is attached to a series of stubs perpendicular to it, as shown in figure 1. The lengths of the stubs and their relative spacing vary along the wire and are designated by b_n and a_n, respectively. We take the quantum wire along the positive X direction and assume that the scatterers are centred at points x_n with respect to some suitable origin. If the lateral cross section of a wire is assumed to be sufficiently small, electrons will occupy only a few lowest quantum states at sufficiently low temperatures. As a result a strong confinement of the motion of the electron in two transverse directions is possible. The electron then moves only along the longitudinal direction. Here, no other scattering potentials are present, except at the intersection of the stub with the wire. The electron is assumed to travel freely along the stub and in the inter-stub zones. The length of the stub may be controlled by tuning the gate voltage [5, 6] and is assumed to be rigid.

Let us consider an electron injected from one side of the structure with wavevector q. The wavefunction in the nth segment (i.e. between the nth and the $(n+1)$th stubs) is written as

$$\psi_n(x) = A_n \exp[\mathrm{i}q(x - x_n)] + B_n \exp[-\mathrm{i}q(x - x_n)]. \tag{1}$$

The wavefunction in the nth stub is given by

$$\phi_n(y) = U_n \exp[\mathrm{i}q(y - b_n)] + V_n \exp[-\mathrm{i}q(y - b_n)]. \tag{2}$$

In writing the above equations, a local coordinate system is chosen for each segment and stub in such a way that the origin is on the left-hand side of the segment [19, 20]. Matching the wavefunctions and their derivatives at the nodes, one easily arrives at the matrix equation:

$$\begin{pmatrix} A_{n+1} \\ B_{n+1} \end{pmatrix} = Q_{n+1,n} \begin{pmatrix} A_n \\ B_n \end{pmatrix} \tag{3}$$

where

$$Q_{n+1,n} = \begin{pmatrix} 1 - \frac{\mathrm{i}\cot(qb_n)}{2} & -\frac{\mathrm{i}\cot(qb_n)}{2} \\ \frac{\mathrm{i}\cot(qb_n)}{2} & 1 + \frac{\mathrm{i}\cot(qb_n)}{2} \end{pmatrix} \begin{pmatrix} \exp(\mathrm{i}qa_n) & 0 \\ 0 & \exp(-\mathrm{i}qa_n) \end{pmatrix}. \tag{4}$$

We now cast the above set of equations into a discrete set of difference equations relating the amplitudes of the wavefunction at any node n with those at the neighbouring nodes $n-1$ and $n+1$. The set of difference equations is given by

$$(E - \epsilon_n)\Psi_n = t_{n,n+1}\Psi_{n+1} + t_{n,n-1}\Psi_{n-1} \tag{5}$$

where $E = 2\cos qa_n$, $\epsilon_n = 2\cos qa_n - \cot qb_n - \cot qa_n - \cot qa_{n+1}$, $t_{n,n+1} = 1/\sin qa_{n+1}$ and $t_{n,n-1} = 1/\sin qa_n$. Equation (5) resembles a typical tight-binding description of a one-dimensional lattice. Ψ_n is the amplitude at the nth node. ϵ_n is equivalent to the magnitude of the on-site potential at the nth site and $t_{n,n\pm1}$ stands for the values of the nearest-neighbour hopping integrals. It should be mentioned here that the presence of the term $E = 2\cos qa_n$ above does not arise automatically. This has been added 'by hand' and subsequently been taken care of in the expression of the on-site term ϵ_n. Here we have defined $a_n = x_n - x_{n-1}$ and $\Psi_n = \psi_n(x_n)$. The set of difference equations (5) thus define an electron which travels in this lattice with a variable energy ranging between $E = \pm 2$. As the conclusions regarding the resonance effects, as well as the transmission coefficient, depend on the difference $E - \epsilon_n$, the addition and subtraction of the term $2\cos qa_n$ do not change the results, although it turns out to be convenient in calculating the transmission coefficient in the present formalism. It is customary to define a 2×2 transfer matrix:

$$M_n = \begin{pmatrix} \frac{(E-\epsilon_n)}{t_{n,n+1}} & -\frac{t_{n,n-1}}{t_{n,n+1}} \\ 1 & 0 \end{pmatrix} \tag{6}$$

such that,

$$\begin{pmatrix} \Psi_{n+1} \\ \Psi_n \end{pmatrix} = M_n \begin{pmatrix} \Psi_n \\ \Psi_{n-1} \end{pmatrix}. \tag{7}$$

3. Short ranged positional correlations and resonance

We define a generalized Fibonacci chain comprising of two different segments L (of length a_L) and S (of length a_S), which are generated according to the rule $L \to LS$ and $S \to L$. The first few generations are: $G_1 = L$, $G_2 = LS$, $G_3 = LSL$ and so on. The stubs of length b_L and b_S are also arranged in a Fibonacci sequence with inter-stub spacings a_L and a_S (figure 2(b)). On the mapped lattice the on-site potentials now assume three distinct values, namely ϵ_α, ϵ_β and ϵ_γ, corresponding to the nodes (sites) flanked by L–L, L–S and S–L elements, respectively. The nearest-neighbour hopping integrals are designated by t_L and t_S, corresponding to the L and S segments (see figure 2). Here

$$\begin{aligned} \epsilon_\alpha &= 2\cos qa_L - \cot qb_L - 2\cot qa_L \\ \epsilon_\beta &= 2\cos qa_L - \cot qb_L - \cot qa_L - \cot qa_S \\ \epsilon_\gamma &= 2\cos qa_L - \cot qb_S - \cot qa_L - \cot qa_S \\ t_L &= 1/\sin qa_L \\ t_S &= 1/\sin qa_S. \end{aligned} \tag{8}$$

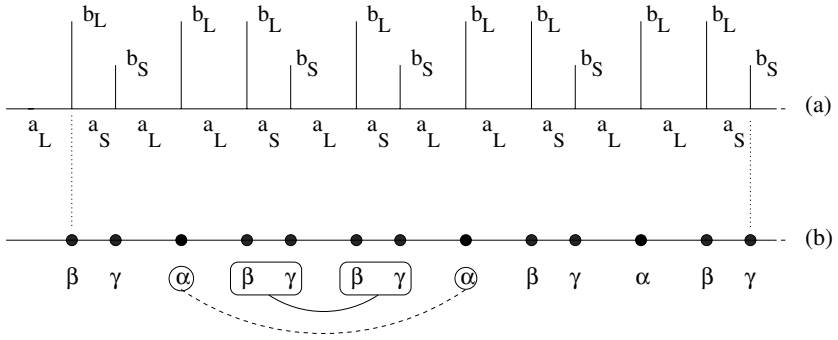

Figure 2. (a) A Fibonacci array of stubs of two different lengths b_L and b_S. The two spacings a_L and a_S are also shown and (b) the equivalent one-dimensional lattice obtained on discretization. The basic building blocks responsible for dimer-like correlations, and hence resonance, are marked by circles (α sites) and boxes ($\beta\gamma$ pairs), respectively.

Accordingly we need to define three different transfer matrices, which are

$$M_\alpha = \begin{pmatrix} \frac{(E-\epsilon_\alpha)}{t_L} & -1 \\ 1 & 0 \end{pmatrix}; \qquad M_\beta = \begin{pmatrix} \frac{(E-\epsilon_\beta)}{t_S} & -\frac{t_L}{t_S} \\ 1 & 0 \end{pmatrix}; \qquad M_\gamma = \begin{pmatrix} \frac{(E-\epsilon_\gamma)}{t_L} & -\frac{t_S}{t_L} \\ 1 & 0 \end{pmatrix}.$$

The standard recursive scheme [21–23] of growing a Fibonacci sequence leads to a recursion relation among the transfer matrices of different generations, namely $M_j = M_{j-2}M_{j-1}$, with $M_1 = M_\alpha$ and $M_2 = M_\gamma M_\beta = M_{\gamma\beta}$. The 'allowed' values of the wavevector q, for a specific set of (b_L, b_S, a_L, a_S), are those for which $|\mathrm{tr}(M_j)| \leqslant 2$ [21–23]. The traces of the transfer matrices M_j are related to each other via a recursion relation [21–23]:

$$x_j = x_{j-1}x_{j-2} - x_{j-3} \tag{9}$$

with $x_1 = \mathrm{Tr}(M_\alpha)$ and $x_2 = \mathrm{Tr}(M_{\gamma\beta}) = \mathrm{Tr}(M_\gamma M_\beta)$. The above 'trace map' leads to a quantity J given by

$$J = \tfrac{1}{4}(x_j^2 + x_{j-1}^2 + x_{j-2}^2 - x_j x_{j-1} x_{j-2} - 4) \tag{10}$$

which remains invariant for all values of $j \geqslant 1$. We are now in a position to discuss resonances in different models of the FWQG array.

3.1. The on-site model

We take $a_L = a_S = a$ and $b_L \neq b_S$. We now have a Fibonacci sequence of equispaced stubs of two different lengths b_L and b_S. This makes $\epsilon_\alpha = \epsilon_\beta \neq \epsilon_\gamma$, which leads to $M_\alpha = M_\beta \neq M_\gamma$. The nearest-neighbour hopping integrals are $t_L = t_S = 1/\sin qa$. For this model the invariant can be worked out, using equations (8)–(10), to be equal to $J = \frac{\sin^2 qa(\cot b_L q - \cot b_S q)}{4}$.

Now, let us choose $qa = (2n + 1)\pi/2$, n being an integer including zero. Then for $b_L = \frac{2m+1}{2n+1}a$ and $b_S = \frac{2p+1}{2n+1}a$, with m, n and p integers, chosen in such a way that $m \neq p$ for a given value of n (so as to ensure that $b_L \neq b_S$), it is simple to work out, using equation (8), that a FQWG structure gets mapped onto a one-dimensional chain with $\epsilon_\alpha = \epsilon_\beta = \epsilon_\gamma = 0$ and $t_L = t_S = \pm 1$. The situation is identical to a periodic sequence of indistinguishable atoms having zero on-site potential and connected to the nearest neighbours by uni-modular hopping integrals. The corresponding wavefunction is extended and perfectly periodic. Thus, even with a FQWG with stubs of lengths b_L and b_S we come across a whole set of values of stub lengths corresponding to a specific value of q, or equivalently an entire set of values of the wavevector

q for a given set of b_L, b_S and a, for which an infinite Fibonacci segment of stubs will sustain extended eigenstates. The individual transfer matrices M_α and $M_{\gamma\beta}$ $(=M_\gamma M_\beta)$ will be equal to $\mathrm{i}\sigma_y$ and $-I$, respectively, where σ_y is the Pauli matrix and I stands for the 2×2 identity matrix. The transmittivity in this will be unity, as can be verified by the method described in section 4. The invariant turns out to be zero for the above combination of parameters.

Before ending this discussion, it may be mentioned that the fact that $M_\alpha = \mathrm{i}\sigma_y$ and $M_{\gamma\beta} = -I$ leads to a map $M_{j+6} = M_j$, $j \geqslant 1$, as is usually seen in a Fibonacci sequence [21–23]. This so-called 'six-cycle' of the matrix map can be traced back to the existence of a pair correlation between certain clusters [24], which is rather straightforward in the on-site model just discussed, but may not be that trivial in other models, as will be clear from the subsequent discussion.

3.2. The transfer model

We now consider a transfer model where stubs of identical length $b_L = b_S = b$ are spaced unequally, i.e. $a_L \neq a_S$. This makes $\epsilon_\alpha \neq \epsilon_\beta = \epsilon_\gamma$ and $t_L \neq t_S$. The invariant is given by $J = \frac{1}{4}\cot^2(bq)\sin^2(qa_L - qa_S)$. In a Fibonacci lattice, the pair of sites $\beta\gamma$ appear side by side, as well as in isolation, separated by the α sites (see figure 2(b)). The α site, on the other hand, never appears pairwise. However, the cluster of sites α–$\beta\gamma$–$\beta\gamma$–α appears locally everywhere (see figure 2(b)). The product transfer matrix across this block is $M_\alpha M_{\gamma\beta} M_{\gamma\beta} M_\alpha$. If we can work out a condition for which the matrix product $M_{\gamma\beta}^2$ at the centre (corresponding to the innermost quadruplet $\beta\gamma$–$\beta\gamma$) turns out to be an identity matrix, the flanking M_α matrices come side by side. Now, by tuning a different parameter of the system, if we can make $M_\alpha^2 = \pm I$ as well, then the local cluster of matrices $M_\alpha M_{\gamma\beta} M_{\gamma\beta} M_\alpha = I$. This is *resonance* in the above local cluster. This happens locally throughout the chain. The clusters of sites $\beta\gamma$–$\beta\gamma$ flanked by the outer pairs α–α form the 'nested' dimers, in the spirit of [24–29]. This leads to a six-cycle in the matrix map, as can be easily verified and has been explained elsewhere [24]. The resonating clusters in the above example are of the minimum possible size and are easily identified at the lowest scale of length, i.e. on the original lattice. Using the RSRG method one can identify such clusters at different scaled versions of the original lattice which correspond to larger sized clusters at the basic length scale [24]. This, however, will need a different relationship between the parameters of the system, such as the length of a stub or the relative spacing between the stubs. We provide the simplest example below. We set

$$qa_L + qa_S = (2n+1)\pi \tag{11}$$

n being an integer. If we now tune the stub length b in such a way that $\cot qb = 2\cot qa_S$, then it is easily seen that $\mathrm{Tr}(M_\alpha) = 0$, leading to $M_\alpha^2 = -I$. The above parametrization yields $\mathrm{Tr}(M_{\gamma\beta}) = 2(2\cos^2 qa_S - 1)$. Therefore, for $qa_S = (2m+1)\pi/4$, $\mathrm{Tr}(M_{\gamma\beta}) = 0$ and hence the product $M_{\gamma\beta} M_{\gamma\beta} = -I$ as well. That is, the requirement $M_\alpha M_{\gamma\beta} M_{\gamma\beta} M_\alpha = I$ is satisfied for the above choices of b, a_L and a_S. The specific values of the wavevector are easily obtained. In fact, for $q = (2n+1)\pi/(a_L + a_S)$ with a_L and a_S suitably chosen, one can come across a whole set of values of b, given by $b = \frac{a_L + a_S}{(2n+1)\pi}\cot^{-1}(2)$, for which resonance will take place. We now present a more general model.

3.3. A mixed model

Let us choose $qa_L = (2n+1)\pi/2$, $qa_S = (2n+1)\pi/6$ and $qb_L = (2m+1)\pi/2$. Here, n and m are integers which may or may not be equal. With these parameters, $M_\alpha = \mathrm{i}\sigma_y$, so that $M_\alpha^2 = -I$. This will happen for an infinite number of values of b_L, depending on m, for fixed values of the wavevector q and the spacings a_L and a_S. The choice of values for b_S remains

open. A straightforward algebra reveals that, for $qb_S = \cot^{-1}(2/\sqrt{3})$, $\mathrm{Tr}(M_{\gamma\beta}) = 0$. This makes $M_{\gamma\beta}M_{\gamma\beta} = -I$. In this case $M_{\gamma\beta} \neq \mathrm{i}\sigma_y$. Here, the minimal resonating clusters are α–$\beta\gamma$–$\beta\gamma$–α as before and are identified easily at the bare length scale.

In order to unravel clusters bigger than α–$\beta\gamma$–$\beta\gamma$–α in the original lattice, one efficient way is to look for a similar cluster in a one-step renormalized lattice [24]. The process of renormalization is well known in the literature [31]. The basic idea is to decimate the β sites so as to obtain a new Fibonacci chain with renormalized values of the parameters. We provide the appropriate recursion relations for the sake of completeness:

$$\begin{aligned}
\epsilon'_\alpha &= \epsilon_\gamma + \frac{t_L^2 + t_S^2}{E - \epsilon_\beta} \\
\epsilon'_\beta &= \epsilon_\gamma + \frac{t_S^2}{E - \epsilon_\beta} \\
\epsilon'_\gamma &= \epsilon_\alpha + \frac{t_L^2}{E - \epsilon_\beta} \\
t'_L &= \frac{t_L t_S}{E - \epsilon_\beta} \\
t'_S &= t_L.
\end{aligned} \tag{12}$$

On this renormalized lattice one can again identify the α sites and the $\beta\gamma$ pairs. Let us stick to the earlier choice of qa_L and qa_S. On the one-step renormalized lattice the condition $\mathrm{Tr}(M_\alpha) = 0$ leads to the requirement

$$(\cot qb_L + \sqrt{3})(\cot qb_S + \sqrt{3}) = 5. \tag{13}$$

As before, we then try to make $\mathrm{Tr}(M_{\gamma\beta}) = 0$ on the renormalized lattice. A simple algebra shows that this can be achieved if we set $qb_L = \cot^{-1}(-8/\sqrt{3}) + n\pi$. This choice of qb_L leads to $qb_S = \cot^{-1}(-2\sqrt{3})$. Thus, for a given value of q, a proper tuning of the stub lengths reveals a correlation between $\beta\gamma$ pairs and α–α pairs on a rescaled version of the lattice. The minimal clusters α–α and $\beta\gamma$–$\beta\gamma$ on the renormalized lattice correspond to the clusters $\beta\gamma$–$\beta\gamma$ and $\alpha\beta\gamma$–$\alpha\beta\gamma$, respectively, in the original (un-renormalized) lattice. This analysis can proceed indefinitely. The above pairs can, in principle, be identified at any stage of renormalization. They will correspond to bigger and bigger clusters on the original lattice. The six-cycle of the matrix map will set in at an appropriate generation of the Fibonacci chain [24]. It may be mentioned here that, in a purely one-dimensional lattice, the six-cycle behaviour of the full matrix map is not easy to locate for different values of the energy of the electron. The FQWG structure, on the other hand, provides a wide range of q values, leading to the cyclic variation of the matrices that can be determined precisely. The adjustment of the stub lengths is, of course, necessary.

In figures 3(b) and (c) we plot $|\psi|^2$ at the nodes for a lattice with 233 stubs. The distributions correspond to a six-cycle wavefunction in the present mixed case. Figure 3(b) represents the case where the positional correlations are explained at the basic length scale by the α–$\beta\gamma$–$\beta\gamma$–α clusters, while figure 3(c) shows the same due to the clusters $\beta\gamma$–$\beta\gamma$ and $\alpha\beta\gamma$–$\alpha\beta\gamma$.

4. Electronic transmission through waveguides

We present the results of our calculation for the on-site model and the transfer model. A more general model can be easily addressed. To calculate the transmission coefficient across a jth generation FQWG array made of equispaced stubs of unequal length, we embed the effective one-dimensional lattice obtained on discretizing the Schrödinger equation into a perfectly

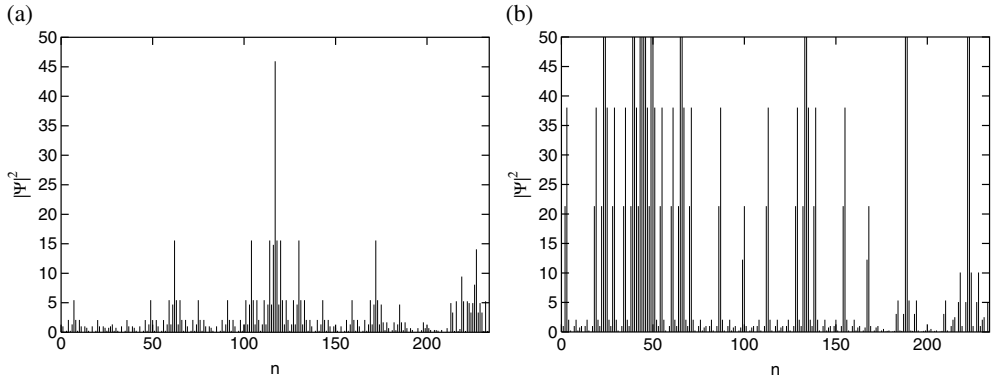

Figure 3. (a) Charge density corresponding to a six-cycle wavefunction where the clusters responsible are: α–α and $\beta\gamma$–$\beta\gamma$. We have chosen $qa_L = \pi/2$, $qa_S = \pi/6$, $qb_L = \pi/2$ and $qb_S = \cot^{-1}(2/\sqrt{3})$. (b) Charge density obtained by resolving the correlations on a one-step renormalized lattice. Here, $qb_L = \cot^{-1}(-8/\sqrt{3})$ and $qb_S = \cot^{-1}(2\sqrt{3})$. Other parameters are the same as in (a). Clusters responsible for resonance are $\beta\gamma$–$\beta\gamma$ and $\alpha\beta\gamma$–$\alpha\beta\gamma$. The charge density in (b) has been displayed within a value of 50 to make the lower values more prominent in comparison to much higher (finite) values, particularly at sites 43–46.

ordered tight binding lattice, acting as a lead. The on-site potential and the nearest-neighbour hopping in the lead are taken to be ϵ_0 and t_0, respectively. In order to be consistent with the parametrization $E = 2\cos qa_L$ we shall fix $\epsilon_0 = 0$ and $t_0 = 1$. Using the trace and anti-trace maps [32, 33], the transmission coefficient for the jth generation chain is given by

$$T(j) = \frac{4\sin^2 qa_L}{(z_j \cos qa_L - y_j)^2 + x_j^2 \sin^2 qa_L} \tag{14}$$

where $x_j = \mathrm{Tr}\, M_j$, $y_j = M_j(2,1) - M_j(1,2)$ and $z_j = M_j(1,1) - M_j(2,2)$, respectively. The so-called 'anti-traces' y_j and z_j obey the following recursion relations [33]:

$$\begin{aligned} y_j &= x_{j-1}y_{j-2} + y_{j-3} \\ z_j &= x_{j-1}z_{j-2} + z_{j-3}. \end{aligned} \tag{15}$$

The initial values of x, y and z are easily obtained from the recursion relations (9) and (13) by noting that $M_1 = M_\alpha = M_\beta$, $M_2 = M_\gamma M_\beta$ and $M_3 = M_\gamma M_\beta M_\alpha$. The transmission coefficient for the on-site model turns out to be a periodic function of qa_L, the period being equal to π. Within a single period the transmission coefficient exhibits both resonance and anti-resonance. In figures 4(a)–(c) we show the variation of the transmittivity for a fifth generation FQWG with $b_L = 2$ and 3 for the fifth and eighth generation chains in the on-site model. In each situation we have taken $a_L = a_S = 1$ and $b_S = 1$. It can be seen that within one period the number of sub-bands is equal to the numerical value of the length of the stub b_L (when b_L has an integral value), measured in units of a_L. Anti-resonance takes place at $qa_L = (2n+1)\pi/2$ whenever $b_L = 2n$, n being an integer. The above values of qa_L turn out to be points of anti-resonance for $b_L = (2n+1)$. Figure 4(c) exhibits the fragmentation in the transmission spectrum as the system size is increased to represent an eighth generation chain. In each figure we also present the variation of the invariant with qa_L. In figure 4(a), the invariant never reaches the value zero, though it diverges at the gap between the two sub-bands within a period. In figure 4(b), however, the invariant becomes zero as the transmission coefficient attains the value unity in the middle of the central sub-band at $qa_L = \pi/2$. In all three figures,

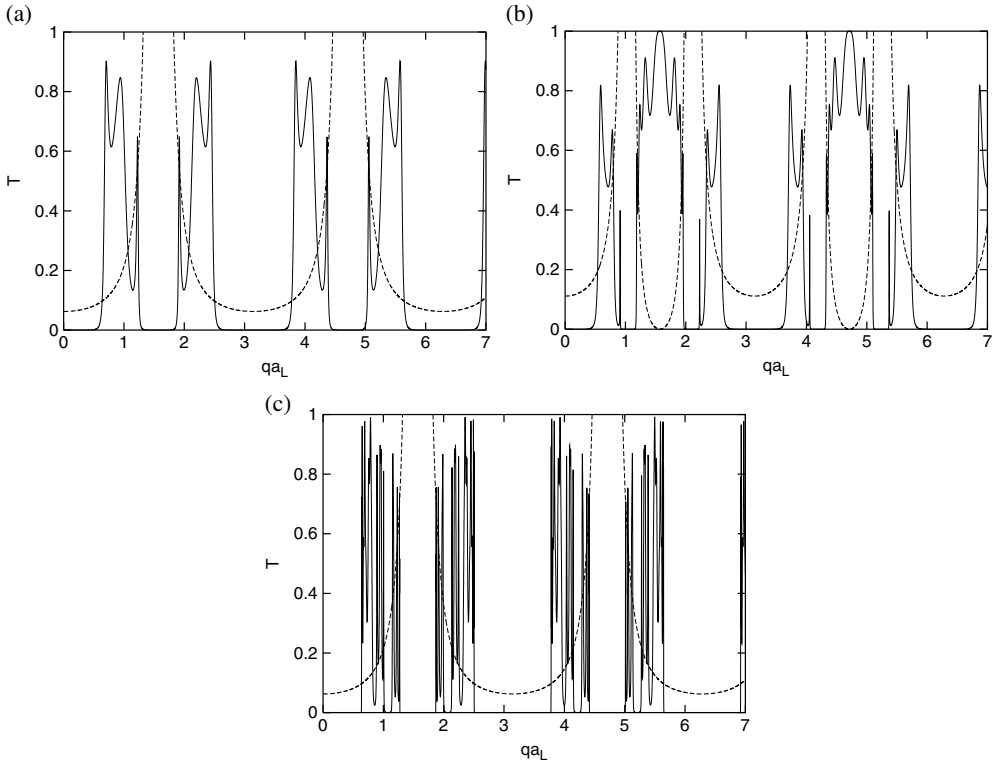

Figure 4. (a) Transmission (full curve) across a fifth generation Fibonacci array (8 stubs). We have chosen $a_L = a_S = 1$, $b_S = 1$ and $b_L = 2$. (b) Same as (a), but with $b_L = 3$. (c) Transmission spectrum for an eighth generation array with 34 stubs. The parameters are the same as in (a). The invariant in each case has been shown by the broken curve.

the transmission coefficient is periodic in qa_L with a period equal to π. This, however, depends on the choice of the stub length.

In figures 5(a) and (b) results for the transfer model are presented for a Fibonacci segment of eighth generation. In either case we have selected $a_L = 1$ and $a_S = 0.5$. The results reveal the sensitivity of the transmission spectrum on the lengths of the stubs. For $b_L = b_S = 0.25$ (in units of a_L) a window of (almost) perfect transmission appears symmetrically on either side of $qa_L = 2\pi$, which is the centre of the spectrum within one period (figure 5(a)). The transmission coefficient in this case has a periodic in qa_L with a period equal to 4π. On increasing the stub length, namely to $b_L = b_S = 1$, the period of the transmission spectrum is reduced to $qa_L = 2\pi$. The central transmission window disappears and gaps open in the transmission spectrum at and around $qa_L = n\pi$. This is shown in figure 5(b) where we plot the spectrum for two periods. Within each period the transmission spectrum exhibits a two sub-band structure. In each figure we also show the variation of the invariant J against qa_L. The invariant remains zero (or vanishingly small) in the central transmission window in figure 5(a) and also in the zones of high transmission ($T \sim 1$) in figure 5(b) and tends to diverge at the gap separating one sub-band from the other in one period (see figure 5(b), for example).

4.1. Commuting matrices and a power-law decay in T

We now present one case where the transmission coefficient in a pure transfer model of a FQWG can be worked out, by hand, to exhibit a power-law decay as the system increases in

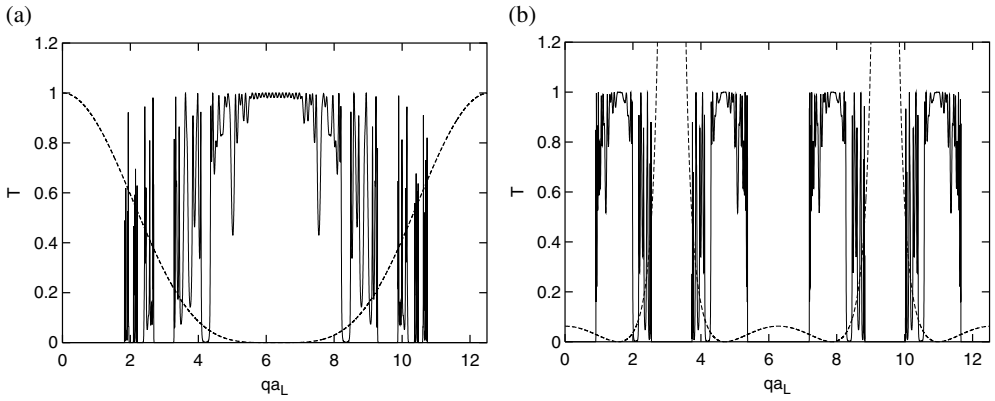

Figure 5. (a) Transmission coefficient for an eighth generation Fibonacci array of stubs in the transfer model. We have taken $a_L = 1$, $a_S = 0.5$ and $b_L = b_S = 0.25$. In (b) $a_L = 1$, $a_S = 0.5$ and $b_L = b_S = 1$. The invariant is once again shown by the broken curve. In each figure, the range of qa_L values has been scanned in an interval of 0.001.

size. This is possible at special values of the wavevector q on simultaneous adjustment of the values of the stub lengths and their relative spacings. Let us choose $q(a_L - a_S) = 2n\pi$ and $b = (2m+1)(a_L - a_S)/(2n)$, where m and n are integers, either equal or unequal. It should be appreciated that choosing $qa_L = 2n\pi + qa_S$ makes $t_L = t_S$ on the equivalent 1D chain while keeping a perfect Fibonacci order in the original arrangement of stubs. This makes $J = 0$ and $[M_\alpha, M_{\gamma\beta}] = 0$. It is then straightforward to work out that, for the above combination of parameters and for a large system size ($j \to \infty$):

$$T(j) \sim \frac{4\sin^2(qa_L)}{4F_j^2[1+\cos(qa_L)]^2 + \sin^2(qa_L)} \tag{16}$$

where F_j is the total number of bonds in the jth generation FQWG segment. Thus, in this special situation the transmission coefficient decays, for a given value of the wavevector, in the manner $T \sim 1/F_j^2$ as the system grows in size. Before ending this section, it should be pointed out that such behaviour has also been observed for special models of a Fibonacci chain by Maciá and Domínguez-Adame [35].

5. Conclusion

We have developed a method of showing the single-electron transport through quasiperiodic quantum waveguide structures. We apply the method to a series of stub-like objects arranged in a Fibonacci sequence. In particular, our emphasis has been on establishing the relationship between the parameters of the system for which local clusters in a Fibonacci sequence conspire to give rise to resonance effects. The cyclic variation of the global transfer matrices are closely linked with these short ranged positional correlations, which can possibly be studied experimentally using such mesoscopic devices. The existence of extended eigenstates has also been discussed. The method is readily applicable to any quasiperiodic or random geometry.

Acknowledgment

One of the authors (AC) gratefully acknowledges CSIR, India for financial support through grant number 03(0944)/02/EMR-II.

References

[1] Kramer B 1991 *Quantum Coherence in Mesoscopic Systems* (*NATO Advanced Study Institute Series B: Physics* vol 254) (New York: Plenum)
[2] Altshuler B L, Lee P A and Webb R A (ed) 1991 *Mesoscopic Phenomenon in Solids* (Amsterdam: North-Holland)
[3] Imry Y 1997 *Introduction to Mesoscopic Physics* (New York: Oxford University Press)
[4] Washburn S and Webb R A 1986 *Adv. Phys.* **35** 375
[5] Sols F, Macucci M, Ravaiol U and Hess K 1989 *Appl. Phys. Lett.* **54** 350
[6] Sols F, Macucci M, Ravaioli U and Hess K 1989 *J. Appl. Phys.* **66** 3892
[7] Datta S and Mclennan M J 1990 *Rep. Prog. Phys.* **53** 1003
[8] van Wees B J, Kouwenhoven L P, Willems E M M, Harmans C J P, Mooij J E, van Houten H, Beenakker C W J, Williams J G and Foxon C T 1991 *Phys. Rev.* B **43** 12431
[9] Datta S 1989 *Superlatt. Microstruct.* **6** 83
[10] Xia J B 1992 *Phys. Rev.* B **45** 3593
[11] Deo P S and Jayannavar A M 1994 *Phys. Rev.* B **50** 11629
[12] Porod W, Shao Z and Lent C S 1993 *Phys. Rev.* B **48** 8495
[13] Kouwenhoven L P, Hekking F W J, van Wees B J, Harmans C J P, Timmering C E and Foxon C T 1990 *Phys. Rev. Lett.* **65** 361
[14] Katsumoto S, Sano N and Kobayashi S 1993 *Solid State Commun.* **85** 223
[15] Ji-Rong S and Ben-Yuan G 1997 *Phys. Rev.* B **55** 4703
[16] Vasseur J O, Daymier P A, Dobrinski L and Choi J 1998 *J. Phys.: Condens. Matter* **10** 8973
[17] Pouthier V and Girardet C 2002 *Phys. Rev.* B **66** 115322
[18] Orellana P A, Dominguez-Adame F, Gomez I and Ladron de Guevara M L 2003 *Phys. Rev.* B **67** 085321
[19] Jin G J, Wang Z D, Hu A and Jiang S S 1999 *J. Appl. Phys.* **85** 1597
[20] Peng R W, Jin G J, Wang Mu, Hu A, Jiang S S and Feng D 2000 *J. Phys.: Condens. Matter* **12** 5701
[21] Bellisard J, Formoso A, Lima R and Testard D 1982 *Phys. Rev.* B **26** 3024
[22] Kohmoto M, Kadanoff L P and Tang C 1983 *Phys. Rev. Lett.* **50** 1870
Ostlund S, Pandit R, Rand D, Schellenhuber H J and Siggia E D 1983 *Phys. Rev. Lett.* **50** 1873
[23] Kohmoto M and Banavar J 1986 *Phys. Rev.* B **34** 563
Bellisard J, Bovier A and Ghez J M 1991 *Commun. Math. Phys.* **135** 379
[24] Chattopadhyay S and Chakrabarti A 2002 *Phys. Rev.* B **65** 184204
[25] Dunlap D H, Wu H-L and Phillips P W 1990 *Phys. Rev. Lett.* **65** 88
[26] Sanchez A, Maciá E and Dominguez-Adame F 1994 *Phys. Rev.* B **49** 147
[27] Datta P K, Giri D and Kundu K 1993 *Phys. Rev.* B **47** 10727
[28] Zhong J X, Xie T, You J Q and Yan J R 1992 *Z. Phys.* B **87** 223
Chakrabarti A, Karmakar S N and Moitra R K 1994 *Phys. Rev.* B **50** 13276
[29] Chakrabarti A, Karmakar S N and Moitra R K 1995 *Phys. Rev. Lett.* **74** 1403
[30] Sire C and Mosseri R 1990 *J. Physique* **51** 1569
[31] Ashraff J A and Stinchcombe R B 1988 *Phys. Rev.* B **37** 5723
Chakrabarti A, Karmakar S N and Moitra R K 1989 *Phys. Rev.* **39** 973
[32] Dulea M, Severin M and Riklund R 1990 *Phys. Rev.* B **42** 3680
[33] Wang X, Grimm U and Schreiber M 2000 *Phys. Rev.* B **62** 14020
[34] Sokoloff J B and José J V 1982 *Phys. Rev. Lett.* **49** 334
[35] Maciá E and Domínguez-Adame F 1996 *Phys. Rev. Lett.* **76** 2957